Acta Crystallographica Section F
Structural Biology and Crystallization Communications
ISSN 1744-3091

Interaction of an echinomycin–DNA complex with manganese ions

Roland Pfoh, Jose A. Cuesta-Seijo and George M. Sheldrick*

Department of Structural Chemistry, University of Göttingen, Tammannstrasse 4, 37077 Göttingen, Germany

Correspondence e-mail: gsheldr@shelx.uni-ac.gwdg.de

Received 19 April 2009
Accepted 23 May 2009

PDB Reference: echinomycin–DNA complex, 3go3, r3go3sf.

The crystal structure of an echinomycin–d(ACGTACGT) duplex interacting with manganese(II) was solved by Mn-SAD using in-house data and refined to 1.1 Å resolution against synchrotron data. This complex crystallizes in a different space group compared with related complexes and shows a different mode of base pairing next to the bis-intercalation site, suggesting that the energy difference between Hoogsteen and Watson–Crick pairing is rather small. The binding of manganese to N7 of guanine is only possible because of DNA unwinding induced by the echinomycin, which might help to explain the mode of action of the drug.

1. Introduction

Echinomycin is found in streptomycetes and belongs to the group of quinoxaline antibiotics that bind to DNA by bisintercalation (Waring & Wakelin, 1974). It consists of two depsipeptides containing D-serine, L-*N*-methylvaline, L-*N*-methylcysteine (L-*S*,*N*-dimethylcysteine in the case of the second peptide strand) and L-alanine with a quinoxaline base attached to D-serine (Dell *et al.*, 1975). The two peptide strands are connected *via* a thioacetal bridge and two ester linkages between D-serine and L-*N*-methylvaline (Fig. 1).

Echinomycin shows activity against vancomycin-resistant enterococci (Kim *et al.*, 2004), hypoxia-inducible factor-1 suppression (Kong *et al.*, 2005), HIV-1 Tat transactivation inhibition (Jayasuriya *et al.*, 2005), antithrombotic activity (Lee *et al.*, 2007) and activity against methicillin-resistant *Staphylococus aureus* (Park *et al.*, 2008).

Footprinting studies indicated that echinomycin mostly binds around 5′-GC, with a preference for AT base pairs at the surrounding sites (Low *et al.*, 1984). Crystal structures of the drug in complex with d(CGTACG), d(GCGTACGC) and d(ACGTACGT) have been reported (Ughetto *et al.*, 1985; Cuesta-Seijo & Sheldrick, 2005; Cuesta-Seijo *et al.*, 2006). In all of them the two quinoxaline bases intercalate around the 5′-GC sites and the depsipeptide backbone is positioned in the minor groove of the DNA. In most of these structures all base pairs next to the 5′-GC site are in the Hoogsteen mode (Cuesta-Seijo & Sheldrick, 2005); only in one structure with d(ACGTACGT) are some of these base pairs Watson–Crick (Cuesta-Seijo *et al.*, 2006).

One of the previous crystal structures of echinomycin in complex with d(ACGTACGT) contained an unexpected metal ion bound to N7 of a guanine (PDB code 2adw). The metal site in this structure was found to be occupied by a mixture of zinc(II) and nickel(II) ions, but it was suspected that it is also capable of binding different transition metals depending on their availability. This assumption was the initial motivation for further crystallization trials. In the presence of Mn^{2+}, a new crystal form was obtained in a different space group and the crystals diffracted to 1.1 Å resolution. This structure is reported here.

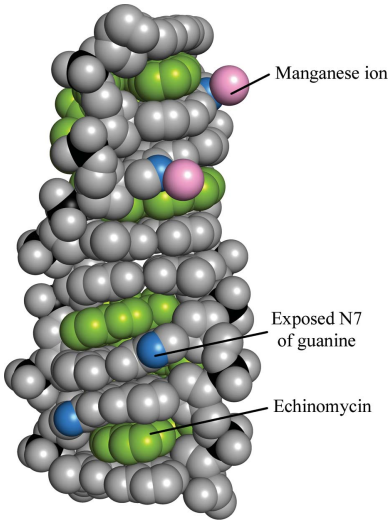

2. Materials and methods

Echinomycin was purchased in lyophilized form from Sigma–Aldrich and d(ACGTACGT) purified by HPLC was purchased from Carl Roth GmbH. Both substances were used without further purification.

2.1. Crystallization

Crystals were grown at 293 K in hanging drops by vapour diffusion. The reservoir solution contained 24%(*v*/*v*) PEG 200, 6%(*w*/*v*) PEG 3350, 16 m*M* manganese(II) chloride, 20 m*M* spermine tetrachloride and 0.1 *M* MES buffer (2-morpholinoethanesulfonic acid) pH 6.0. The DNA–drug solution contained 0.21 m*M* d(ACGTACGT) (single-strand concentration), 0.25 m*M* echinomycin and 50%(*v*/*v*) methanol; it was prepared by mixing echinomycin dissolved in methanol with aqueous oligonucleotide solution in a 1:1 ratio at room temperature and incubating for 6 d at 277 K. Hanging drops prepared from 20 µl DNA–drug solution and 1 µl reservoir solution were equilibrated against 500 µl reservoir solution. After one week spherulites appeared in the crystallization drop and after two months colourless bar-shaped tetragonal crystals had grown to dimensions of 0.1 × 0.1 × 0.3 mm. For data collection at 100 K, the crystals were flash-cooled in liquid nitrogen. The mother liquor around the crystals proved to be sufficient for cryoprotection.

2.2. Data collection, structure solution and refinement

The data sets used for this project are listed in Table 1. The in-house data set Home2 was integrated with *SAINT* (Bruker AXS, Madison, Wisconsin, USA) and the other two data sets were integrated with *XDS* (Kabsch, 1993). Data scaling was performed with *SADABS* (Bruker AXS, Madison, Wisconsin, USA) and space-group determination and preparation of the SAD data were performed with *XPREP* (Bruker AXS, Madison, Wisconsin, USA).

The structure was solved using the anomalous dispersion of manganese with a highly redundant in-house SAD data set (Home2) measured with a Bruker SMART6000 16 megapixel CCD detector on a three-circle goniometer. With a resolution cutoff of 2.1 Å, *SHELXD* (Schneider & Sheldrick, 2002; Sheldrick, 2008) found three manganese sites with a relative occupancy of 1.0:0.4:0.1, of which the first two turned out to be real. Phase extension to 1.0 Å by 200 cycles of density modification using *SHELXE* (Sheldrick, 2002, 2008) produced an easily interpretable map (Fig. 2*a*). We could find only four previous reports of phasing by Mn-SAD (Dauter *et al.*, 2002; Ramagopal *et al.*, 2003; Stevenson *et al.*, 2004; Salgado *et al.*, 2005), even though manganese is not uncommon in enzymes and has significant anomalous scattering at the Cu $K\alpha$ wavelength.

For refinement, a high-resolution data set collected at SLS (Switzerland) that contained many overloaded reflections was merged with a weaker 2.25 Å in-house data set (Home1) collected with a MAR345 detector which was free of overloads. It was found that this data set

Table 1
Data-collection, phasing and refinement statistics.

Values in parentheses are for the outermost resolution shell.

	SLS	Home1	Home2
Crystal data			
Space group	$P4_12_12$	$P4_12_12$	$P4_12_12$
Unit-cell parameters (Å)			
a	26.54	26.43	26.46
c	162.32	162.27	162.44
Diffraction data			
Beamline	PXII at SLS	Rotating anode	Rotating anode
Wavelength (Å)	1.00000	1.54178	1.54178
Resolution limit (Å)	1.10	2.23	1.65
Total reflections	130500	37857	175783
Unique reflections	23140	3325	7727
Completeness (%)	92.2 (76.5)	99.5 (99.5)	97.7 (89.4)
Multiplicity	5.20 (2.17)	11.39 (11.59)	22.75 (9.31)
$I/\sigma(I)$	24.06 (4.44)	23.93 (12.85)	41.42 (9.75)
$R_{\rm int}$† (merged Friedel pairs)	3.28 (20.19)	7.42 (21.53)	4.78 (19.02)
$R_{\rm p.i.m.}$† (merged Friedel pairs)	1.42 (13.09)	2.28 (8.81)	0.91 (5.61)
$R_{\rm anom}$†			5.72 (15.78)
Data merging (SLS–Home1)			
$R_{\rm merge}$ (SLS–Home1) (%)	15.38		
Completeness (%)	94.3 (76.3)		
To 1.25 Å resolution	99.7		
Phasing			
Resolution (Å)			2.1
Pseudo-free CC (*SHELXE*) (%)			70.13
Refinement			
Reflections used	22400		
Resolution (Å)	1.1		
R_1 [$F_o > 4\sigma(F_o)$] (%)	15.6		
$R_{\rm free}$ [$F_o > 4\sigma(F_o)$] (%)	19.1		
R.m.s. deviation			
Distances (Å)	0.018		
Angles (°)	2.5		

† $R_{\rm int} = 100\sum_{hkl}|I_{hkl} - \langle I_{hkl}\rangle|/\sum_{hkl}(I_{hkl})$, $R_{\rm p.i.m.} = 100\sum_{hkl}\{[1/(N-1)]^{1/2}\times|I_{hkl} - \langle I_{hkl}\rangle|\}/\sum_{hkl}(I_{hkl})$, $R_{\rm anom} = 200\sum_{hkl}|I_{hkl} - I_{-h-k-l}|/\sum_{hkl}(I_{hkl} + I_{-h-k-l})$ and $R_{\rm merge} = 100\sum_{hkl}|I_{1,hkl} - I_{2,hkl}|/\sum_{hkl}\langle I_{hkl}\rangle$, where N is the number of equivalent reflections in each group of equivalents.

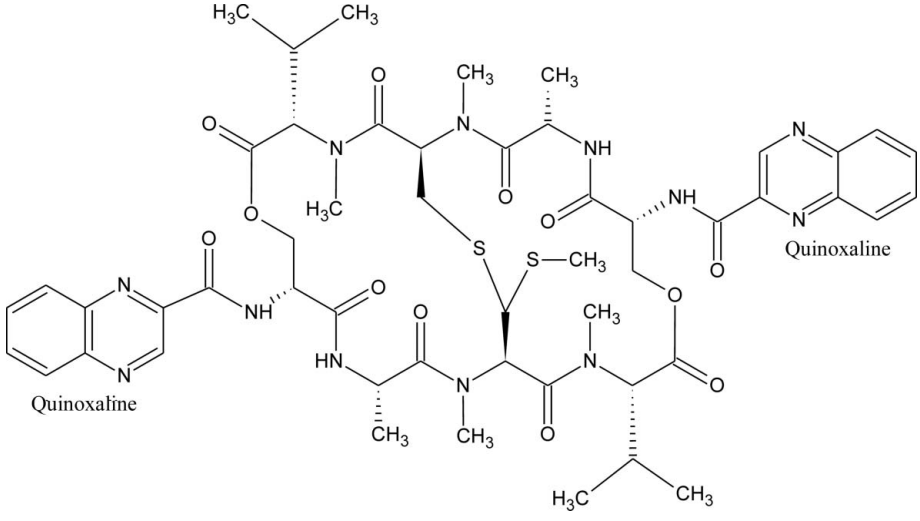

Figure 1
Schematic diagram of echinomycin.

produced a better merging R value and better final R values than merging the synchrotron data with data set Home2. The merged data set was almost complete to 1.25 Å resolution but beyond that resolution some reflections were missing; the completeness in the last resolution shell (1.20–1.10 Å) was 76.5%. The structure was refined anisotropically against the merged data with *SHELXL* (Sheldrick & Schneider, 1997; Sheldrick, 2008) to R_1 = 15.6% and R_{free} = 19.1% (Fig. 2*b*).

3. Results and discussion

3.1. Base pairing

In agreement with all previous crystal structures, the bases enclosed by echinomycin [base pairs C(2)–G(107), G(3)–C(106), C(6)–G(103) and G(7)–C(102)] show Watson–Crick pairing. Most bases flanking the bisintercalation site show Hoogsteen pairing, except for the terminal base pair A(1)–T(108), which exhibits Watson–Crick pairing. A summary of the available crystal structures of d(ACGTACGT)–echinomycin complexes is given in Table 2. Three of the four show different patterns of base pairing. The AT pairs seem to be able to adopt either Hoogsteen or Watson–Crick pairing independently of each other, except that the two central base pairs [T(4)–A(105) and A(5)–T(104)] either both adopt Hoogsteen or both adopt Watson–Crick pairing. This result further confirms the intrinsic flexibility of the complex suggested by NMR data (Gilbert & Feigon, 1991).

3.2. Interactions with manganese(II) ions

The metal site described by Cuesta-Seijo *et al.* (2006) is also found in this structure. Two guanine bases interact with manganese ions, in particular atom N7 of residue G(107) and atom N7 of residue G(3). In the first case, the octahedral coordination of manganese is completed by the phosphate group of a symmetry-related molecule and four water molecules. The distance between manganese and N7 of residue G(107) is 2.31 Å. The second manganese site is not fully occupied. Since this ion lies close to a symmetry equivalent of itself, the occupancy was set to 50%, which is approximately the value found by *SHELXD* (see above). The distance to N7 of residue G(3) is 2.38 Å. Water molecules surrounding the ion do not appear clearly in the difference map, probably because they are involved in disorder caused by the half-occupied metal site, and only two of them were modelled. In the crystallization drop, the ratio of manganese ions to DNA–echinomycin duplexes was about 8:1.

Table 2
Base-pairing types for the known d(ACGTACGT)–echinomycin X-ray structures.

WC stands for Watson–Crick and HG for Hoogsteen base pairing.

		PDB code 2adw		
Base pair	PDB code 1xvn	Duplex 1	Duplex 2	PDB code 3go3 (this work)
A(1)–T(108)	HG	HG	HG	WC
C(2)–G(107)	WC	WC	WC	WC
G(3)–C(106)	WC	WC	WC	WC
T(4)–A(105)	HG	WC	HG	HG
A(5)–T(104)	HG	WC	HG	HG
C(6)–G(103)	WC	WC	WC	WC
G(7)–C(102)	WC	WC	WC	WC
T(8)–A(101)	HG	WC	HG	HG

It has been suggested by Gao *et al.* (1993) that direct binding between cobalt(II) and N7 of intrahelical guanine is not possible in A-form and B-form DNA because there would not be enough room for the waters of the hydration shell of the metal ion in the deep major groove. This assumption was expanded to other bivalent transition metals (Ni^{2+}, Zn^{2+}) and confirmed by several crystallographic studies (Abrescia *et al.*, 2002; Labiuk *et al.*, 2003). In these studies, interactions with transition metals were observed for terminal or flipped-out bases but not for intrahelical bases. Mg^{2+} usually binds to N7 of guanine in B-DNA through a water molecule in its coordination sphere, but transition-metal cations such as Mn^{2+}, Co^{2+}, Ni^{2+}, Cu^{2+} and Zn^{2+} are softer Lewis acids and so have a higher affinity for nitrogen. In the PDB, direct contacts between manganese and nonterminal intrahelical nucleobases can only be found in DNA–protein complexes in which the DNA is significantly bent by the protein. An example would be the nucleosome core particle (*e.g.* PDB code 2nzd; Ong *et al.*, 2007), in which a DNA duplex is wrapped around a histone protein octamer. The situation is completely different for Z-DNA, where the major groove is flat and the bases are more exposed; Gao *et al.* (1993) observed direct binding between Co^{2+} and N7 of intrahelical guanine with an average bond distance of 2.3 Å.

Fig. 3 illustrates the unwinding in the DNA–echinomycin complex (Fig. 3*a*) in comparison with B-DNA (Fig. 3*b*). The B-DNA structure

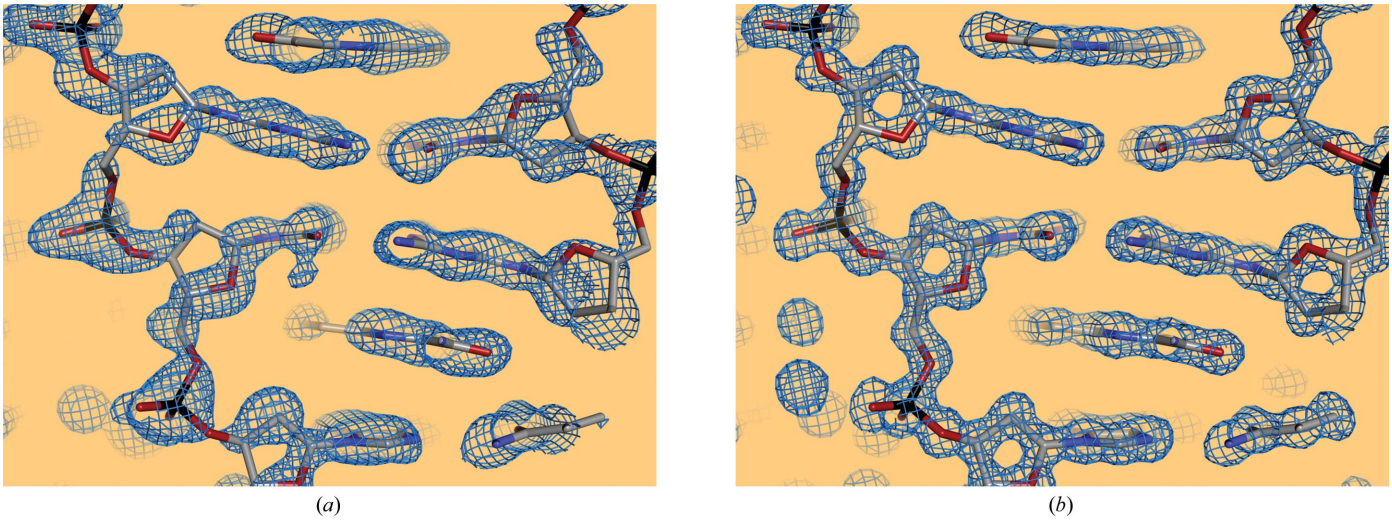

(*a*) (*b*)

Figure 2
Experimental map (*a*) and map after final refinement (*b*), both contoured at a 1σ level.

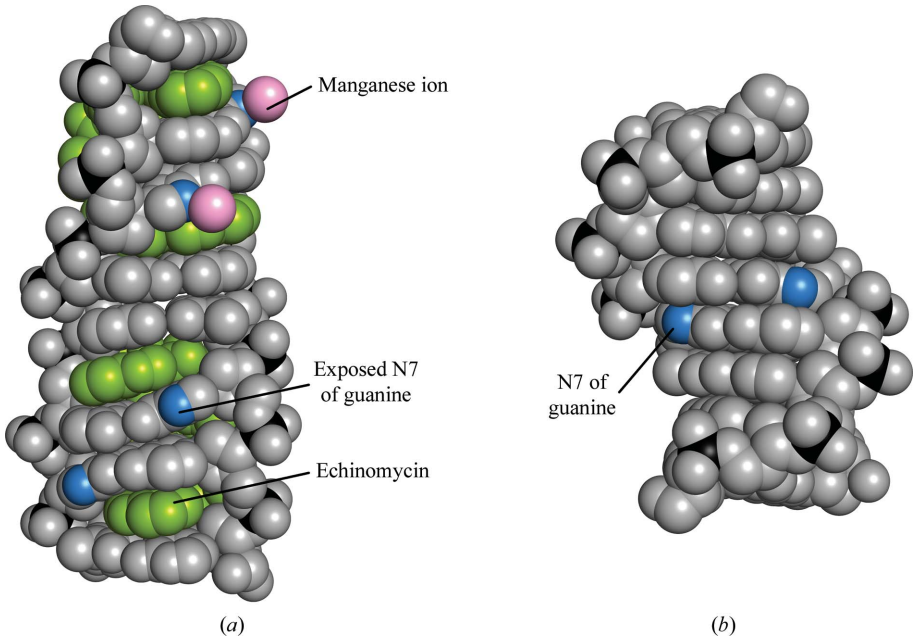

Figure 3
Space-filling models of the DNA–echinomycin complex (*a*) and B-DNA (*b*). Echinomycin is shown in green, P atoms in black, N7 of guanines in blue and manganese ions in pink. The hydration waters of manganese have been omitted for clarity.

(Chiu & Dickerson, 2000; PDB code 1en3) of the decamer d(CCA-ACGTTGG) was shortened to an octamer by omitting the terminal residues in order to compare the overall helical twist of the two structures. The B-DNA structure is twisted from the top to the bottom base pair by more than 360°, whereas the DNA–drug complex is twisted from A(1) to T(8) by only about 120°. Some base pairs are actually oriented parallel to each other in this structure. The major groove in B-DNA is wide and deep; in the DNA–drug complex it is no longer recognizable. Some parts of it seem to be on the verge of a left-handed helix geometry, which can be recognized by looking at the two phosphate groups at the upper left side. In both structures the N7 atoms belonging to nonterminal guanine bases are highlighted in blue. In the DNA–drug complex the two upper N7 atoms interact directly with Mn^{2+}. It can be seen that all four N7 atoms are very exposed in this structure, whereas in B-DNA the N7 of guanine is more hidden at the side of the major groove, mainly by the phosphate group but also by the sugar and the base from the cytosine residue positioned above it.

4. Conclusions

A new crystal form of the echinomycin–d(ACGTACGT) complex was obtained with manganese(II) ions, pushing the resolution limit for this complex from 1.50 to 1.10 Å. The overall structure presented here is similar to previous examples, but with a small difference in the mode of base pairing. The observed interactions between N7 of the intrahelical guanine and the Mn^{2+} ion show that the binding to echinomycin allows reactions of nucleobases in the major groove of DNA. We suggest that part of the high biological activity of echinomycin arises from reactions (*e.g.* alkylations) of N7 of guanine facilitated by DNA unwinding. Echinomycin could act as a catalyst and might amplify the effect of alkylating agents.

1.5 Mn atoms proved to be sufficient to phase a structure with 472 non-H atoms on a home source. This is probably a consequence of the fact that transition-metal complexes adopt a rigid structure, resulting in well defined metal positions. In the case of bent DNA (*e.g.* in protein–DNA complexes) or RNA, transition-metal ions such as Ni^{2+}, Zn^{2+}, Mn^{2+} and Co^{2+} would also bind to intrahelical nucleobases and could be used for phasing with Mn^{2+} and Co^{2+} using Cu $K\alpha$ radiation. Additionally, they might improve crystallization and resolution limits by facilitating intermolecular contacts.

We thank the personnel of beamline PXII of SLS (Switzerland) for assistance with the data collections. We are grateful to the Deutsche Forschungsgemeinschaft (grant Sh 15/5-1) and the Fonds der Chemischen Industrie for support.

References

Abrescia, N. G. A., Huynh-Dinh, T. & Subirana, J. A. (2002). *J. Biol. Inorg. Chem.* **7**, 195–199.
Chiu, T. K. & Dickerson, R. E. (2000). *J. Mol. Biol.* **301**, 915–945.
Cuesta-Seijo, J. A. & Sheldrick, G. M. (2005). *Acta Cryst.* D**61**, 442–448.
Cuesta-Seijo, J. A., Weiss, M. S. & Sheldrick, G. M. (2006). *Acta Cryst.* D**62**, 417–424.
Dauter, Z., Dauter, M. & Dodson, E. (2002). *Acta Cryst.* D**58**, 494–506.
Dell, A., Williams, D. H., Morris, H. R., Smith, G. A., Fenney, J. & Roberts, G. C. K. (1975). *J. Am. Chem. Soc.* **97**, 2497–2502.
Gao, Y.-G., Sriram, M. & Wang, A. H.-J. (1993). *Nucleic Acids Res.* **21**, 4093–4101.
Gilbert, D. E. & Feigon, J. (1991). *Biochemistry*, **20**, 2483–2494.
Jayasuriya, H., Zink, D. L., Polishook, J. D., Bills, G. F., Dombrowski, A. W., Genilloud, O., Pelaez, F. F., Herranz, L., Quamina, D., Lingham, R. B., Danzeizen, R., Graham, P. L., Tomassini, J. E. & Singh, S. B. (2005). *Chem. Biodivers.* **2**, 112–122.
Kabsch, W. (1993). *J. Appl. Cryst.* **26**, 795–800.
Kim, J.-B., Lee, G.-S., Kim, Y.-B., Kim, S.-K. & Kim, Y.-H. (2004). *Int. J. Antimicrob. Agents*, **24**, 613–615.
Kong, D., Park, E. J., Stephen, A. G., Calvani, M., Cardellina, J. H., Monks, A., Fisher, R. J., Shoemaker, R. H. & Melillo, G. (2005). *Cancer Res.* **65**, 9047–9055.
Labiuk, S. L., Delbaere, L. T. J. & Lee, J. S. (2003). *J. Biol. Inorg. Chem.* **8**, 715–720.
Lee, Y.-K., Park, J. H., Moon, H. T., Lee, D. Y., Yun, J. H. & Byun, Y. (2007). *Biomaterials*, **28**, 1523–1530.

Low, C. M. L., Drew, H. R. & Waring, M. J. (1984). *Nucleic Acids Res.* **12**, 4865–4879.
Ong, M. S., Richmond, T. J. & Davey, C. A. (2007). *J. Mol. Biol.* **368**, 1067–1074.
Park, Y.-S., Shin, W.-S. & Kim, S.-K. (2008). *J. Antimicrob. Chemother.* **61**, 163–168.
Ramagopal, U. A., Dauter, M. & Dauter, Z. (2003). *Acta Cryst.* D**59**, 868–875.
Salgado, P. S., Walsh, M. A., Laurila, M. R. L., Stuart, D. I. & Grimes, J. M. (2005). *Acta Cryst.* D**61**, 108–111.
Schneider, T. R. & Sheldrick, G. M. (2002). *Acta Cryst.* D**58**, 1772–1779.
Sheldrick, G. M. (2002). *Z. Kristallogr.* **217**, 644–650.
Sheldrick, G. M. (2008). *Acta Cryst.* A**64**, 112–122.
Sheldrick, G. M. & Schneider, T. R. (1997). *Methods Enzymol.* **277**, 319–343.
Stevenson, C. E. M., Tanner, A., Bowater, L., Bornemann, S. & Lawson, D. M. (2004). *Acta Cryst.* D**60**, 2403–2406.
Ughetto, G., Wang, A. H.-J., Quigley, G. J., van der Marel, G. A., van Boom, J. H. & Rich, A. (1985). *Nucleic Acids Res.* **13**, 2305–2323.
Waring, M. J. & Wakelin, L. P. G. (1974). *Nature (London)*, **252**, 653–657.